SUPPLEMENTAL MATERIAL FOR

Anion Ordered and Ferroelectric Ruddlesden-Popper Oxynitride $Ca_3Nb_2N_2O_5$ for Visible-Light-Active Photocatalysis

Gaoyang Gou,[*,†] Min Zhao,[†] Jing Shi,[†] Jaye K. Harada,[‡] and James M. Rondinelli[*,‡]

†*Frontier Institute of Science and Technology, and State Key Laboratory for Mechanical Behavior of Materials, Xi'an Jiaotong University, Xi' an 710049, People's Republic of China*

‡*Department of Materials Science and Engineering, Northwestern University, 2220 Campus Drive, Evanston, Illinois 60208-3108, USA*

E-mail: gougaoyang@xjtu.edu.cn; jrondinelli@northwestern.edu

Calculated crystal structures for $CaNbO_2N$

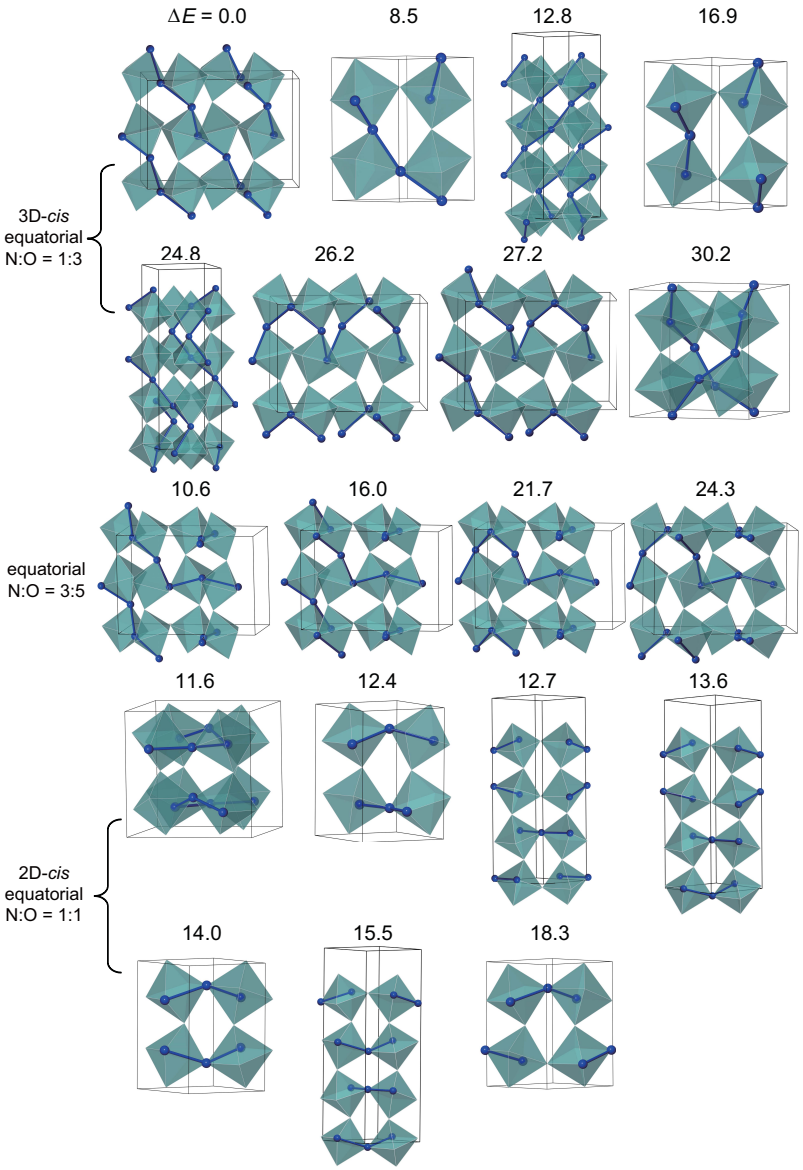

Figure S1: Our optimized low-lying configurations for $CaNbO_2N$ phase with *Pnma* symmetry. The total energy for each configuration (in meV/f. u.) relative to the most stable structure are also presented. N anions are represented by blue balls. *A*-site Ca, *B*-site Nb cations and O anions are omitted for clarity.

Table S1: Calculated crystallographic parameters for the most stable $CaNbO_2N$ 3D-*cis* configuration (1×2×1 of primary cell).

a = 5.62 Å, b = 10.97 Å, c = 7.88 Å, α = 90.0°, β = 90.0°, γ = 89.6°			
Atom	x	y	z
Ca	0.0338	0.4964	0.2371
Ca	0.0315	0.0015	0.2487
Ca	0.9369	0.0103	0.7435
Ca	0.9432	0.5120	0.7421
Ca	0.4713	0.2507	0.7461
Ca	0.4707	0.7501	0.7445
Ca	0.5533	0.2582	0.2424
Ca	0.5663	0.7583	0.2469
Nb	0.4752	0.0051	-0.0052
Nb	0.5049	0.5113	-0.0022
Nb	0.0055	0.2524	0.9860
Nb	-0.0021	0.7567	0.9841
Nb	0.4954	0.0050	0.4849
Nb	0.4958	0.5048	0.4854
Nb	0.0217	0.2585	0.4965
Nb	0.0261	0.7575	0.4939
O	0.5341	0.4515	0.7556
O	0.5413	0.9508	0.7553
O	0.9571	0.2019	0.2564
O	0.9732	0.6998	0.2561
O	0.2826	0.3488	0.0551
O	0.3126	0.8433	0.0476
O	0.6928	0.1472	0.9570
O	0.1948	0.5947	0.9532
O	0.7771	0.3915	0.0575
O	0.8055	0.8972	0.0555
O	0.7031	0.1437	0.5555
O	0.7073	0.6440	0.5539
O	0.8011	0.4008	0.4517
O	0.8037	0.8985	0.4539
O	0.1978	0.0971	0.5505
O	0.2050	0.5992	0.5566
N	0.4812	0.0395	0.2506
N	0.0086	0.2916	0.7516
N	0.1896	0.0954	0.9597
N	0.3091	0.8469	0.4622
N	0.4663	0.5431	0.2524
N	0.0147	0.7913	0.7509
N	0.7065	0.6468	0.9642
N	0.3056	0.3464	0.4624

Table S 2: Calculated crystallographic parameters for the most stable $CaNbO_2N$ 2D-*cis* configuration ($\sqrt{2} \times \sqrt{2} \times 1$ of primary cell).

a = 7.87 Å, b = 7.89 Å, c = 7.79 Å, α = 90.0°, β = 90.0°, γ = 91.3°			
Atom	x	y	z
Ca	0.0064	0.9801	-0.0027
Ca	0.5014	0.4989	-0.0039
Ca	0.9648	0.0611	0.4973
Ca	0.4698	0.5423	0.4960
Ca	0.9551	0.5303	0.4890
Ca	0.4522	0.0478	0.4939
Ca	0.0161	0.5109	0.9890
Ca	0.5190	-0.0066	-0.0061
Nb	0.7201	0.2666	0.7532
Nb	0.2504	0.7752	0.7421
Nb	0.7364	0.7557	0.7446
Nb	0.2284	0.2569	0.7516
Nb	0.7208	0.2660	0.2420
Nb	0.2511	0.7746	0.2532
Nb	0.2348	0.2855	0.2446
Nb	0.7428	0.7843	0.2516
O	0.7715	0.3419	0.0020
O	0.2705	0.8308	0.0023
O	0.1997	0.6993	0.5020
O	0.7006	0.2104	0.5023
O	0.8128	0.8075	0.5009
O	0.2907	0.3047	0.5007
O	0.1583	0.2338	0.0009
O	0.6805	0.7365	0.0007
O	0.9863	0.7373	0.8083
O	0.9879	0.3225	0.6966
O	0.2723	0.5244	0.8091
O	0.7874	0.0294	0.8073
O	0.9849	0.3040	0.3083
O	0.9833	0.7187	0.1966
O	0.6989	0.5168	0.3091
O	0.1837	0.0119	0.3073
N	0.4879	0.8061	0.3016
N	0.4820	0.2234	0.2006
N	0.2705	0.5186	0.2004
N	0.7794	0.0208	0.2026
N	0.4832	0.2351	0.8016
N	0.4892	0.8179	0.7006
N	0.7007	0.5227	0.7004
N	0.1917	0.0205	0.7026

Soft phonon modes and structural instabilities

Table S3: The calculated soft-mode frequencies (in cm^{-1}) for two primary structural distortions ($a^-a^-c^0$ and $a^0a^0c^+$ NbO_4N_2 octahedral rotations) in the high-symmetry 2D, 3D-*cis* $CaNbO_2N$, and Ruddlesden-Popper 2D-*cis* $Ca_3Nb_2N_2O_5$ phases.

	$a^-a^-c^0$	$a^0a^0c^+$
3D-*cis* $CaNbO_2N$	i 207.1	i 228.2
2D-*cis* $CaNbO_2N$	i 217.6	i 177.3
2D-*cis* $Ca_3Nb_2N_2O_5$	i 213.6	i 186.3

We choose the distortion-free $CaNbO_2N$ configurations with 2D, 3D-*cis* O/N arrangement, and Ruddlesden-Popper 2D-*cis* $Ca_3Nb_2N_2O_5$ structure as the high-symmetry references, from which the soft phonon modes with imaginary frequencies and the associated structural instabilities can be identified. After performing zone-center phonon calculations, two primary unstable phonon modes are identified in both high-symmetry $CaNbO_2N$ and $Ca_3Nb_2N_2O_5$ phases, which correspond to out-of-phase $a^-a^-c^0$ and in-phase $a^0a^0c^+$ NbO_4N_2 octahedral rotations. Especially, the calculated imaginary phonon frequencies for $a^-a^-c^0$ and $a^0a^0c^+$ modes in high-symmetry 2D-*cis* $Ca_3Nb_2N_2O_5$ phase are very close to those in 2D-*cis* $CaNbO_2N$ (Table S3). After freezing soft-modes into the high-symmetry phases, followed by structural relaxations, the stable $CaNbO_2N$ and $Ca_3Nb_2N_2O_5$ structures that display pronounced $a^-a^-c^+$ octahedral rotations are obtained.

Calculated crystal structures for Ruddlesden-Popper $Ca_3Nb_2N_2O_5$

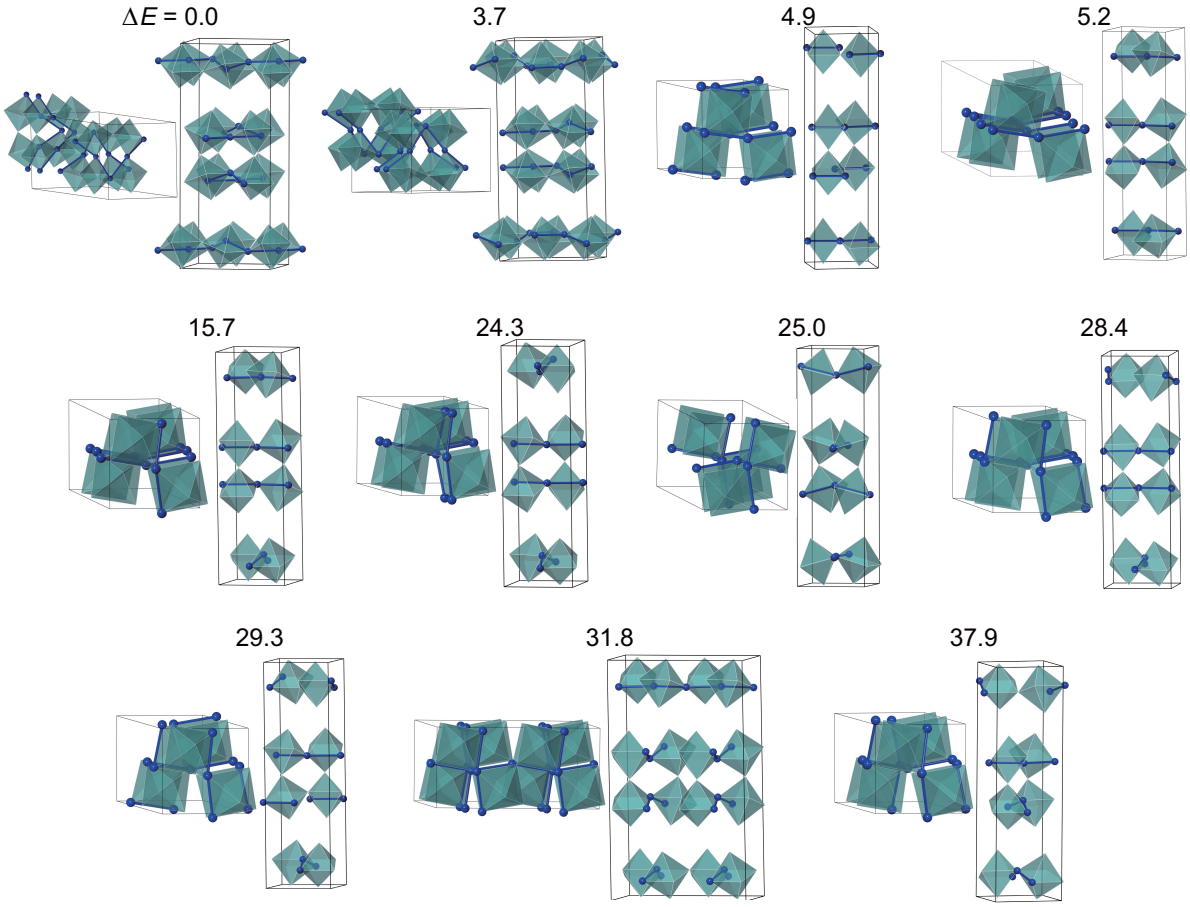

FigureS2: Side and top views of the optimized low-lying configurations for Ruddlesden-Popper $Ca_3Nb_2N_2O_5$. The total energy for each configuration (in meV/f. u.) relative to the most stable structure are also presented. All stable $Ca_3Nb_2N_2O_5$ configurations have 2D-*cis* type O/N arrangement. N anions are represented by blue balls. *A*-site Ca, *B*-site Nb cations and O anions are omitted for clarity.

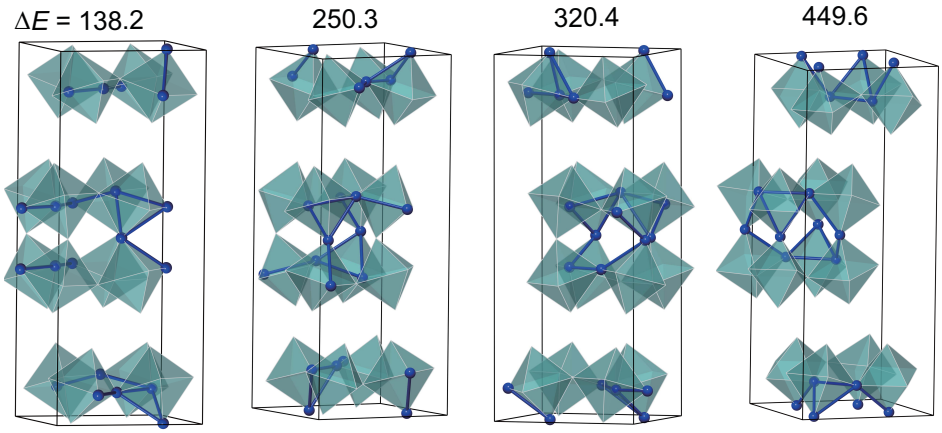

FigureS3: Side view for unfavorable Ruddlesden-Popper $Ca_3Nb_2N_2O_5$ structural configurations where $4a$ apical sites in the middle of perovskite blocks are occupied by N. The total energy for each configuration (in meV/f. u.) is given relative to the most stable $Ca_3Nb_2N_2O_5$ structure. N anions are represented by blue balls. A-site Ca, B-site Nb cations and O anions are omitted for clarity.

Table S4: Calculated crystallographic parameters for the most stable Ruddlesden-Popper $Ca_3Nb_2N_2O_5$ configuration ($\sqrt{2} \times \sqrt{2} \times 1$ of primary cell).

a = 7.830 Å, b = 7.833 Å, c = 19.331 Å, α = 90.0 °, β = 90.0 °, γ = 89.0 °							
Atom	x	y	z	Atom	x	y	z
Ca	0.7665	0.2687	0.5001	O	0.7100	0.9979	0.1210
Ca	0.2896	0.7679	0.5002	O	0.9988	0.2019	0.8795
Ca	0.2781	0.2759	0.5001	O	0.9961	0.2098	0.1232
Ca	0.7596	0.7686	0.5000	O	0.9596	0.7436	0.6226
Ca	0.0245	0.0095	0.9979	O	0.7491	0.4603	0.3779
Ca	0.5286	0.5251	0.9990	O	0.2541	0.9433	0.3793
Ca	0.0164	0.5360	0.9996	O	0.7490	0.4601	0.6227
Ca	0.5189	0.0130	0.9997	O	0.2540	0.9429	0.6214
Ca	0.7355	0.2220	0.3111	O	0.9594	0.7436	0.3780
Ca	0.2118	0.7194	0.3089	O	0.7119	0.3017	0.2017
Ca	0.2142	0.2144	0.6900	O	0.7173	0.3081	0.7990
Ca	0.7237	0.7262	0.6888	O	0.2202	0.8130	0.2009
Ca	0.2151	0.2149	0.3101	O	0.2220	0.8202	0.7991
Ca	0.7241	0.7260	0.3115	O	0.3013	0.2162	0.7994
Ca	0.7354	0.2215	0.6893	O	0.3018	0.2222	0.2008
Ca	0.2109	0.7182	0.6917	O	0.8230	0.7133	0.7981
Ca	0.9771	0.9704	0.8113	O	0.8200	0.7168	0.2017
Ca	0.4724	0.4627	0.8070	O	0.9715	0.0471	0.7003
Ca	0.9691	0.4630	0.1903	O	0.4664	0.5722	0.7013
Ca	0.4745	0.9817	0.1898	O	0.5637	0.9700	0.2986
Ca	0.9653	0.4621	0.8105	O	0.5641	0.9704	0.7022
Ca	0.4669	0.9788	0.8104	O	0.9726	0.0464	0.2995
Ca	0.9763	0.9713	0.1872	O	0.4669	0.5704	0.2986
Ca	0.4687	0.4652	0.1912	O	0.0540	0.4594	0.2995
Nb	0.7326	0.2531	0.0993	O	0.0539	0.4587	0.7012
Nb	0.2572	0.7451	0.1027	O	0.7015	0.7788	0.9992
Nb	0.2515	0.2500	0.9012	O	0.2802	0.6885	0.9998
Nb	0.7384	0.7454	0.8946	O	0.0383	0.9141	0.5000
Nb	0.2485	0.2336	0.0987	O	0.5371	0.4517	0.5002
Nb	0.7495	0.7318	0.1031	O	0.1690	0.2845	0.9998
Nb	0.7355	0.2371	0.8991	O	0.4337	0.0262	0.5003
Nb	0.2472	0.7321	0.8949	O	0.7834	0.1796	0.0006
Nb	0.9848	0.9958	0.5977	N	0.4597	0.2485	0.3819
Nb	0.4838	0.4981	0.6032	N	0.7108	0.9951	0.8803
Nb	0.0052	0.4818	0.4013	N	0.4966	0.2914	0.9206
Nb	0.4972	0.0052	0.3969	N	0.7492	0.0323	0.5791
Nb	0.0047	0.4813	0.5993	N	0.2467	0.5432	0.5803
Nb	0.4969	0.0050	0.6038	N	0.0446	0.2417	0.4205
Nb	0.9851	0.9963	0.4022	N	0.2470	0.5434	0.4201
Nb	0.4840	0.4980	0.3968	N	0.4598	0.2485	0.6189
O	0.9234	0.5273	0.5003	N	0.4938	0.2949	0.0796
O	0.9980	0.7994	0.0798	N	0.2843	0.9991	0.0797
O	0.8060	0.4949	0.9195	N	0.7948	0.4957	0.0810
O	0.2920	0.9990	0.9216	N	0.5004	0.7017	0.8803
O	0.0029	0.7955	0.9193	N	0.2035	0.4971	0.8789
O	0.5492	0.7476	0.4194	N	0.0444	0.2416	0.5797
O	0.5493	0.7478	0.5808	N	0.7494	0.0325	0.4212
O	0.1944	0.5034	0.1205	N	0.4998	0.7084	0.1183

Polarization switching path in Ruddlesden-Popper $Ca_3Nb_2N_2O_5$

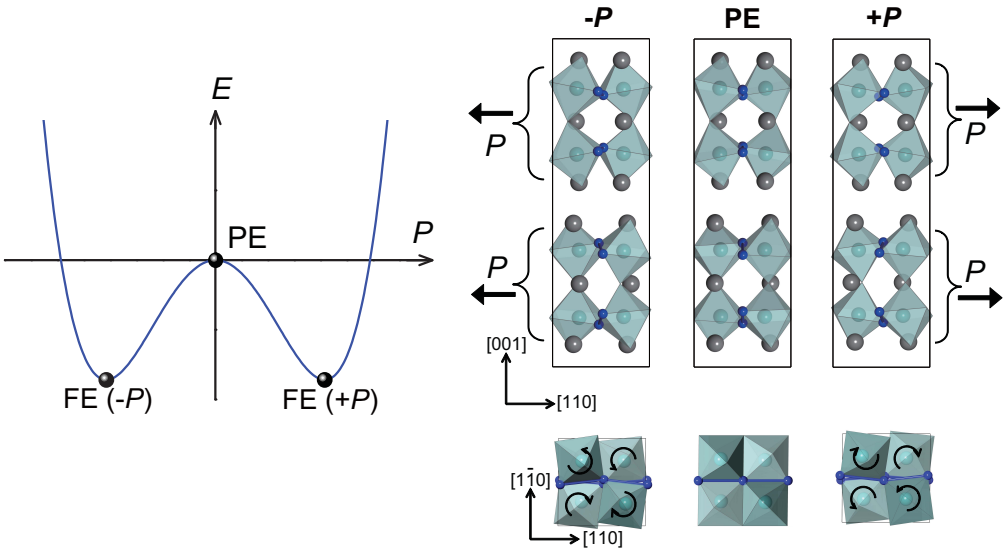

Figure S4: One possible polarization switching path obtained from one ferroelectric 2D-*cis* $Ca_3Nb_2N_2O_5$ configuration. Polarization switching between two FE phases of opposite P is accompanied by reversal of $a^0a^0c^+$ octahedral rotation mode. As a result, the saddle point along the path corresponds to PE phase with $a^-a^-c^0$ rotation mode only. The overall energy barrier (FE-PE energy difference) is calculated to be 64 meV/f. u. for ferroelectric $Ca_3Nb_2N_2O_5$. Black arrows indicate the direction of octahedral rotation along the out-of-plane direction and the effective polarization for each perovskite block. O anions are omitted for clarity.

Electronic structure calculations using HSE hybrid functional

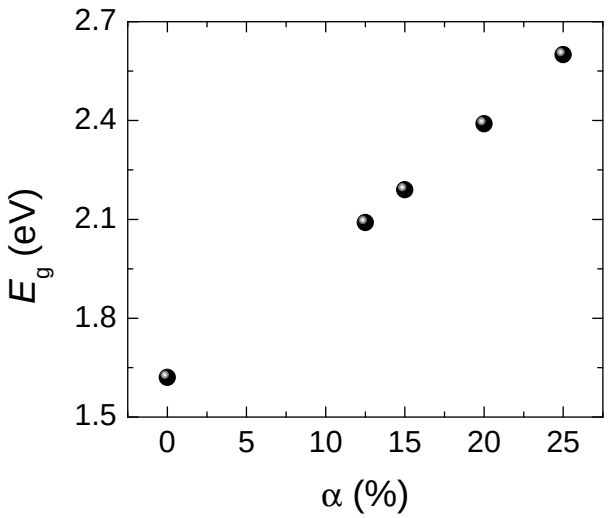

Figure S5: Our calculated band gap (E_g) of $CaNbO_2N$ 3D-*cis* configuration as a function of the percent exact exchange α included in the HSE functional.

It is known that HSE predicted band gap for a semiconducting or insulating material is usually highly dependent on the parameter α, which determines the percentage of exact exchange included in HSE fucntional. Shown in Figure S5 is our calculated band gap of $CaNbO_2N$ 3D-*cis* configuration as a function of the percent exact exchange included in HSE electronic structure calculation, where the band gap increases linearly with increasing α. To reach agreement with the experimentally determined $CaNbO_2N$ band gap (2.1 eV),[1] we selected the parameter $\alpha = 0.125$ (produced a band gap of 2.09 eV) for HSE calculation of all Perovskite oxynitride compounds investigated in this work.

Figure S6 summarizes the project density of states (PDOS) for the stable 3D-, 2D-*cis* $CaNbO_2N$ and Ruddlesden-Popper 2D-*cis* $Ca_3Nb_2N_2O_5$ configurations, calculated using HSE (with 12.5 % exact exchange) and PBEsol functionals respectively. Compared to PBEsol electronic structures, HSE calculations can predict larger energy band gaps for all three configurations, but do not alter distribution of PDOS for Nb-4*d*, O-2*p* and N-2*p* states in both valence and conduction bands.

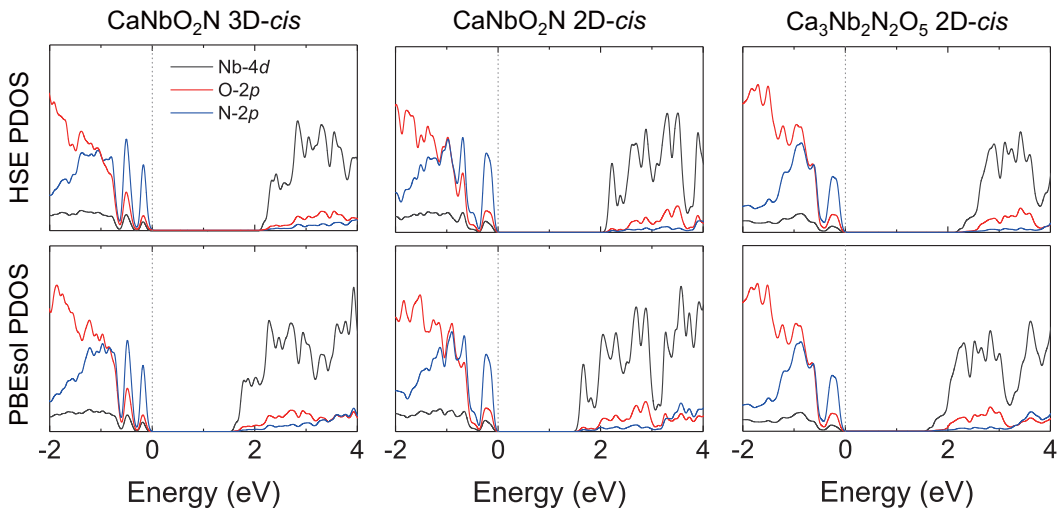

Figure S6: HSE (with 12.5 % exact exchange) and PBEsol calculated project density of states (PDOS) for the ground-state stable $CaNbO_2N$ configurations with 3D-, 2D-*cis* O/N arrangement and Ruddlesden-Popper 2D-*cis* $Ca_3Nb_2N_2O_5$ structure. The Fermi energy level is set at 0 eV, indicated by the broken line.

References

(1) Kim, Y.-I.; Woodward, P. M.; Baba-Kishi, K. Z.; Tai, C. W. Characterization of the Structural, Optical, and Dielectric Properties of Oxynitride Perovskites AMO_2N (A = Ba, Sr, Ca; M = Ta, Nb). *Chem. Mater.* **2004**, *16*, 1267–1276.